

# Peculiarities of Magnetoresistive Properties of Nanostructured $(\text{Ni}_{80}\text{Fe}_{20})_x\text{Au}_{1-x}$ Thin Films: Concentration and Annealing Effects

I.M. PAZUKHA\*, S.R. DOLGOV-GORDIICHUK, A.M. LOHVYNOV,  
K.V. TYSCHENKO AND O.V. PYLYPENKO

*Sumy State University, Sumy 40007, Ukraine*

Received: 24.03.2023 & Accepted: 15.05.2023

Doi: [10.12693/APhysPolA.144.69](https://doi.org/10.12693/APhysPolA.144.69)

\*e-mail: [i.pazuha@aph.sumdu.edu.ua](mailto:i.pazuha@aph.sumdu.edu.ua)

In this report, peculiarities of magnetoresistive properties of nanostructured  $(\text{Ni}_{80}\text{Fe}_{20})_x\text{Au}_{1-x}$  thin films containing from 10 to 60 at.% of Au were investigated. We focus on the samples with a thickness of 45 nm fabricated by the method of electron-beam co-evaporation. The influence of Au atoms concentration and the annealing process within the temperature range from 300 to 700 K on the microstructure, magnitude, and nature of magnetoresistive effects has been discussed. The analysis of electronographic studies showed that both face-centered cubic  $\text{Ni}_3\text{Fe}$  and Au phases are visible in the diffraction images. Upon varying thin film compositions and annealing conditions, the phase state does not change. At the same time, magnetoresistive properties of thin films demonstrated a strong dependence on both the concentration of sample components and annealing conditions. Samples after deposition showed typical giant magnetoresistance behavior at 20–46 at.% of Au, which is also typical for samples annealed at 400 and 500 K. The transition to the anisotropic nature of magnetoresistance occurs upon annealing at 500 K.

topics: thin-film, co-evaporation, annealing, magnetoresistance

## 1. Introduction

Nanostructured thin films based on ferromagnetic alloy  $\text{Ni}_{80}\text{Fe}_{20}$  and noble metal Au are a typical magnetic nanostructure that consists of nanometer-sized ferromagnetic granules embedded into a non-magnetic conduction matrix. The study of such nanostructures is much more popular due to their transport phenomena, magnetic and magnetoresistive properties [1–3]. Notice, in particular, that the discovery of the giant magnetoresistance (GMR) effect in granular nanostructures opened new opportunities for the production of sensing devices [4–6]. As GMR in such structures arises because of spin-dependent scattering of conduction electrons either within magnetic granules or at the interfaces of magnetic granules and non-magnetic matrix, the magnetic granule size and inter-granule distance are very important parameters [7]. These parameters significantly depend on the concentration of sample components and annealing conditions [8, 9].

At present, there is a huge amount of experimental investigations concerning the magnetoresistive properties (MR) analysis of granular

nanostructures  $(\text{Ni}_{80}\text{Fe}_{20})_x\text{Me}_{1-x}$ , where Me is a noble metal [10–12]. Nevertheless, the MR properties of nanostructured  $(\text{Ni}_{80}\text{Fe}_{20})_x\text{Au}_{1-x}$  thin film in correlation with structural properties have not been widely studied. It is especially relevant for granular nanostructures in the condition of the size effect appearance. Nonetheless, the size effect can be significant in MR when the thickness of the samples is comparable to the average size of a single-domain granule [13, 14]. So in this article, we focused on the nanostructured thin  $(\text{Ni}_{80}\text{Fe}_{20})_x\text{Au}_{1-x}$  containing from 10 to 60 at.% of Au with a relatively low thickness of 45 nm. To determine the stability of magnetoresistive properties upon annealing, the investigations of MR behavior during the heat treatment at incrementally increasing temperatures within the range from 300 to 700 K were done.

## 2. Experimental detail

Nanostructured  $(\text{Ni}_{80}\text{Fe}_{20})_x\text{Au}_{1-x}$  thin films with thickness  $d = 45$  nm were sputtered on the glass-ceramic substrates at room temperature by the co-evaporation technique. The  $\text{Ni}_{80}\text{Fe}_{20}$  target

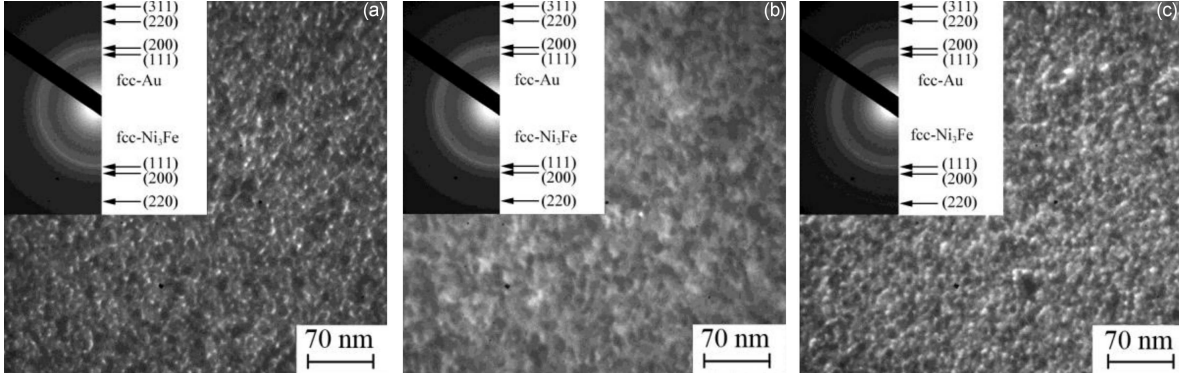


Fig. 1. Bright field TEM images and diffractions patterns in the insert for nanostructured  $(\text{Ni}_{80}\text{Fe}_{20})_x\text{Au}_{1-x}$  thin films at  $d = 45$  nm and  $c_{\text{Au}} = 52$  at.% (a), 40 at.% (b), and 20 at.% (c) after deposition.

(the weight ratio of Ni and Fe is 4:1) and Au target (99.99% purity) were separately installed on two independently controlled electron-beam evaporators in a vacuum chamber with a base pressure of  $10^{-4}$  Pa. All substrates were placed in a vacuum chamber in a row. In such a location, each substrate was placed at a different distance from  $\text{Ni}_{80}\text{Fe}_{20}$  and Au sources. The condensation rate was 0.1 nm/s for  $\text{Ni}_{80}\text{Fe}_{20}$  and Au. The thickness was monitored by two “*in situ*” quartz resonators. As a result, a series of samples with a concentration of Au atoms in the range of 10–60 at.% was obtained in one deposition run.

Composition analysis of thin films was done using a scanning electron microscope (TESCAN VEGA3) equipped with an energy-dispersive detector to perform the X-ray spectrometry.

The magnetoresistive properties were measured using a software–hardware complex with current-in-plane geometries in an external magnetic field from 0 to 600 mT. All measurements were performed at room temperature. The measuring current was  $I = 1$  mA. The value of longitudinal (magnetic field in the sample plane and parallel to current) and transverse (magnetic field in the sample plane and perpendicular to current) magnetoresistance have been calculated by equation

$$\text{MR} = \frac{R(B) - R(B_0)}{R(B_0)}, \quad (1)$$

where  $R(B)$  is the current value of resistance in the magnetic field  $B$ ;  $R(B_0)$  is the value of resistance of the sample in the  $B_0$  field.

For investigation of the annealing temperature effect on magnetoresistive properties, samples were annealed at incrementally increasing temperatures within the range of  $T_{\text{ann}} = 300\text{--}700$  K, staying at each temperature for 20 min. The annealing was carried out in a vacuum chamber with a pressure of  $10^{-3}$  Pa.

A transmission electron microscope (TEM-125K) was employed to determine the phase state and crystal structure of the samples.

### 3. Results and discussion

#### 3.1. Phase state and crystal structure

Since the phase state determines the peculiarities of magnetoresistive properties of thin films, the corresponding research was carried out for nanostructured  $(\text{Ni}_{80}\text{Fe}_{20})_x\text{Au}_{1-x}$  thin films after condensation and annealing. Diffraction patterns and bright field TEM images for  $(\text{Ni}_{80}\text{Fe}_{20})_x\text{Au}_{1-x}$  thin films with various concentrations of Au atoms are shown in Fig. 1. It is clear that all samples showed diffraction rings corresponding to two face-centered cubic (fcc) lattices, namely, fcc- $\text{Ni}_3\text{Fe}$  and fcc-Au. In addition, the diffraction ring (200) Au overlaps with (111)  $\text{Ni}_3\text{Fe}$ , which leads to an increase in the intensity of the second ring. Besides, for the film with low and higher Au atoms concentration, the phase state is the same. The lattice parameters are 0.354 nm for fcc- $\text{Ni}_3\text{Fe}$  and 0.406 nm for fcc-Au. Note that according to [15–17], the components of the samples (Ni, Fe, and Au) can already mix at the stage of their formation at room temperature. As a result of this mixing, solid solutions or intermetallic compounds based on Ni and Au or Fe and Au can be formed. This is accompanied by a change in the lattice parameter values or the appearance of additional peaks in the diffraction images. At the same time, we do not find any additional diffraction peaks or other evidence of the formation of solid solutions or compounds. It can therefore be concluded that nanostructured  $(\text{Ni}_{80}\text{Fe}_{20})_x\text{Au}_{1-x}$  thin films have a two-phase state fcc- $\text{Ni}_3\text{Fe} + \text{fcc-Au}$ .

The analysis of the morphology of magnetic granules also allows us to carry out a more comprehensive investigation of MR results. According to the data of electron microscopic studies, the structure of the thin films at  $c_{\text{Au}} = 52$  at.% in an as-deposited state consists of magnetic granules surrounded by an Au matrix (Fig. 1a). The granules with size from 5 to 15 nm are uniformly dispersed in the Au matrix. With the subsequent reduction

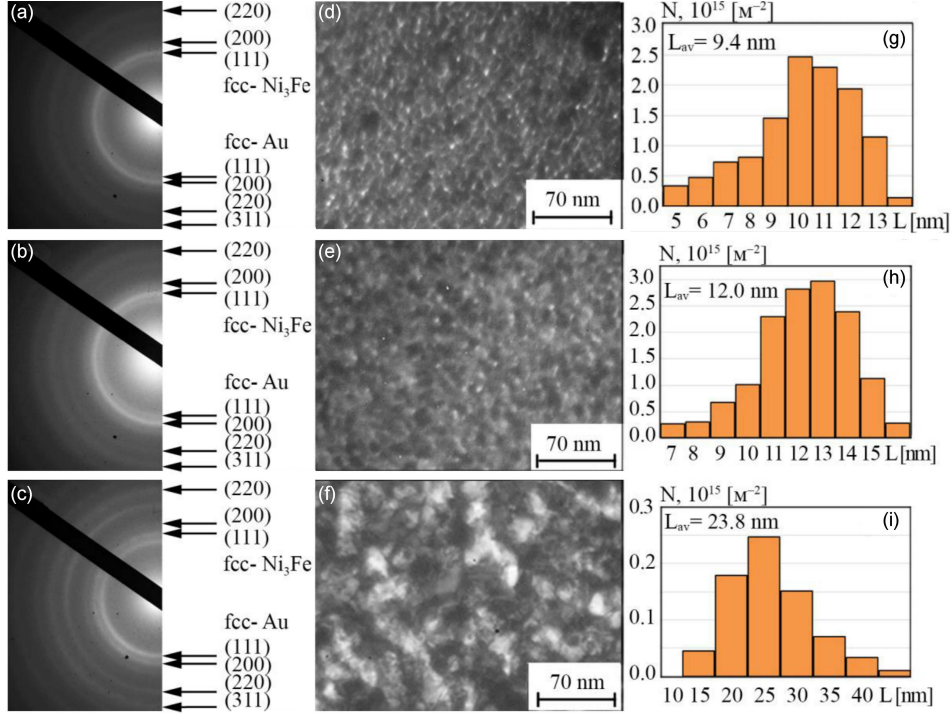


Fig. 2. Diffraction patterns (a)–(c), bright field TEM images (d)–(f), and the grain size distribution (g)–(i) for  $(\text{Ni}_{80}\text{Fe}_{20})_x\text{Au}_{1-x}$  thin films at  $c_{\text{Au}} = 30$  at.% and  $d = 45$  nm after deposition (a), (d), (g) and heat treatment at 500 K (b), (e), (h) and 700 K (c), (f), (i).

of the Au concentration to 40 at.% (Fig. 1b) and 20 at.% (Fig. 1c), the grain size decreases monotonically.

The modification diffraction and TEM images after annealing at 500 and 700 K are shown in Fig. 2. Panels (a)–(c) reveal that the phase state did not change by annealing and corresponds to fcc- $\text{Ni}_3\text{Fe}$ + fcc-Au with a corresponding slight increase of lattice parameters to 0.355 nm and 0.407 nm. It should be noted that the phase state of annealed films remains the same within the whole range of Au atom concentration.

An evaluation of the crystal structure after annealing for  $(\text{Ni}_{80}\text{Fe}_{20})_x\text{Au}_{1-x}$  thin films at  $c_{\text{Au}} = 30$  at.% is displayed in Fig. 2, panels (d)–(f). Based on the bright-field TEM images, the grain size distribution was plotted (Fig. 2, panels (g)–(i)). It is clear that ferromagnetic granules weakly grow, and their average size  $L_{av}$  increases from 9.4 nm in the as-deposited state to 12 nm after annealing to 500 K. At the same time, the increase of  $T_{ann}$  up to 700 K stimulates an intensive recrystallization process and more significant grains grows ( $L_{av} = 23.8$  nm) compared to as-deposited films.

### 3.2. Magnetoresistive properties

The field dependences of the longitudinal (LMR) and transverse (TMR) magnetoresistance at different Au concentrations for  $(\text{Ni}_{80}\text{Fe}_{20})_x\text{Au}_{1-x}$  thin

films are shown in Fig. 3. At low Au concentration ( $c_{\text{Au}} \leq 20$  at.%), the  $\text{MR}(B)$  dependences have anisotropic character (Fig. 3a). The reason for anisotropic magnetoresistance appearing is the formation of ferromagnetic metal infinity clusters and occurrence of the magnetic anisotropy in the film plane. The part of the magnetic granules that grow during the condensation process touches each other to form a multi-domain magnetic structure. Hence, the samples of this composition show properties close to  $\text{Ni}_{80}\text{Fe}_{20}$  film alloy [18]. In the concentration range  $c_{\text{Au}} = 21$ –36 at.% (Fig. 3b and c), the shape of the LMR and TMR curves transforms. For both geometries, the MR value increases linearly with the field, without reaching saturation, and almost coincides. So, in this case, the effect of giant magnetoresistance (GMR) is observed. As stated before, the GMR is conditional by a spin-dependent scattering of electrons either within or at the interfaces of magnetic granules and non-magnetic matrix. Therefore, the size of granules and their distribution in the non-magnetic matrix are important for GMR realization. It was shown [19, 20] that single-domain ferromagnetic granules affect the giant magnetoresistance for nanostructures based on ferromagnetic alloys  $\text{Ni}_x\text{Fe}_{1-x}$  and Cu or Au. As a rule, the magnitude of GMR reaches a maximum value as the systems approach the percolation threshold. Note the percolation parameters are non-universal and sensitive to the ferromagnetic granule distribution and the conductive matrix topology [8]. Also, the

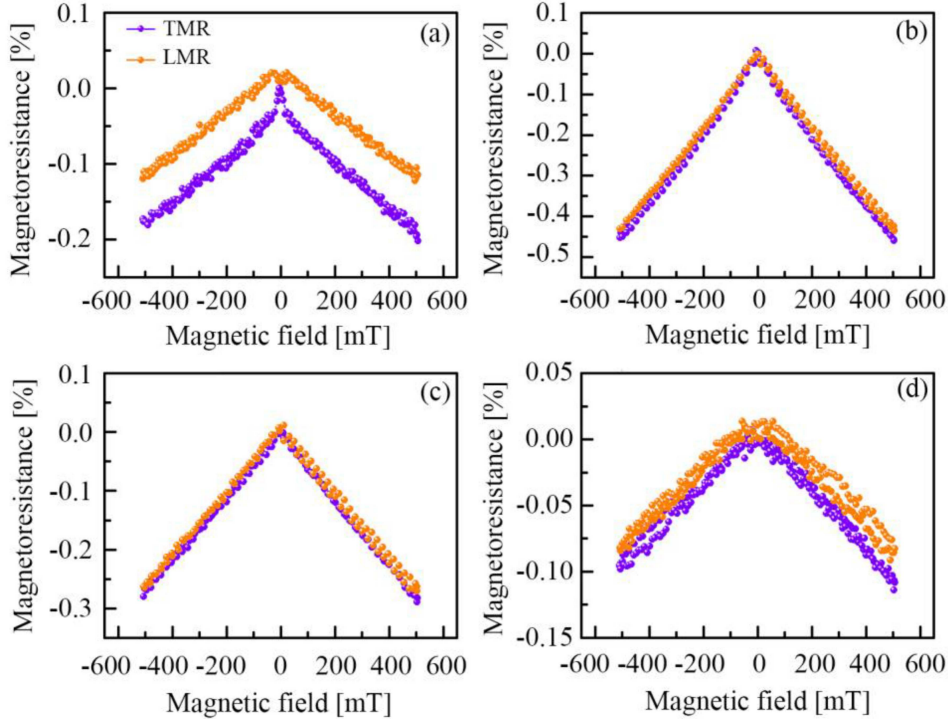


Fig. 3. Field dependences of longitudinal (LMR) and transverse (TMR) magnetoresistance for as-deposited  $(\text{Ni}_{80}\text{Fe}_{20})_x\text{Au}_{1-x}$  thin films at  $d = 45$  nm and  $c_{\text{Au}} = 20$  (a), 30 (b), 36 (c), and 40 at.% (d).

preparation method has a great influence on the magnetoresistive properties of nanostructured thin films. With increasing  $c_{\text{Au}}$  in the range from 21 to 30 at.%, the ferromagnetic granules gradually become smaller, causing an increase in the number of single-domain granules. It leads to growth in the probability of spin-dependent electron scattering and an improvement of the GMR effect. A further increase in  $c_{\text{Au}}$  up to 40% leads to the formation of the cupola-like shape of MR vs  $B$  curves (Fig. 3d). Field dependences of longitudinal and transverse magnetoresistance show negligible hysteresis and do not saturate in fields up to 600 mT. This behavior indicates the presence of superparamagnetic granules that interacted weakly. With further increase in  $c_{\text{Au}}$  up to 40%, their density and the distance between them increase significantly, which leads to falling in GMR.

The dependence of the longitudinal and transverse magnetoresistance as a function of the Au concentration for as-deposited  $(\text{Ni}_{80}\text{Fe}_{20})_x\text{Au}_{1-x}$  thin films is presented in Fig. 4. LMR and TMR values increase with the Au atom concentration and reach the maximum of 0.45% at  $c_{\text{Au}} = 30$  at.%, after which they decrease dramatically with further growth of  $c_{\text{Au}}$ . This result correlates with data presented in [11], where it was reported that for a sample based on  $\text{Ni}_{80}\text{Fe}_{20}$  and Cu, the maximum GMR value is observed at  $c_{\text{Cu}} = 34$  at.%. At the same time, from previous studies [19, 21, 22], it is known that for as-deposited thin films based on ferromagnetic alloys  $\text{Ni}_x\text{Fe}_{1-x}$  and noble metal,

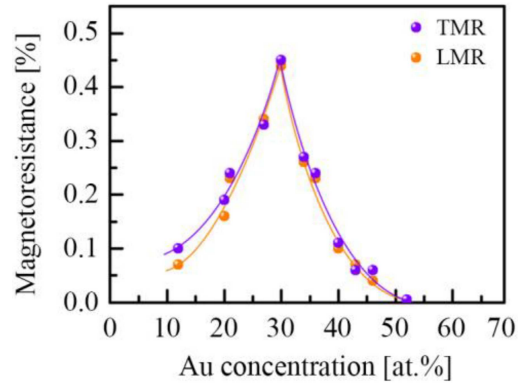


Fig. 4. Longitudinal (LMR) and transverse (TMR) magnetoresistance as a function of the Au atom concentration for as-deposited  $(\text{Ni}_{80}\text{Fe}_{20})_x\text{Au}_{1-x}$  thin films at  $d = 45$  nm.

GMR reaches a maximum in the concentration range of noble metal  $60 \leq c_{\text{Au}} \leq 80$  at.%. In our opinion, the shift of the maximum with the concentration dependence of GMR has been associated with the decrease in the total thickness of thin films. As a result, the growth of ferromagnetic granules is limited in one of the directions in comparison with thicker films. The annealing effect on magnetoresistive properties of nanostructured  $(\text{Ni}_{80}\text{Fe}_{20})_x\text{Au}_{1-x}$  thin film is discussed by the example of the sample with the highest observed value of GMR ( $c_{\text{Au}} = 30$  at.%). The field

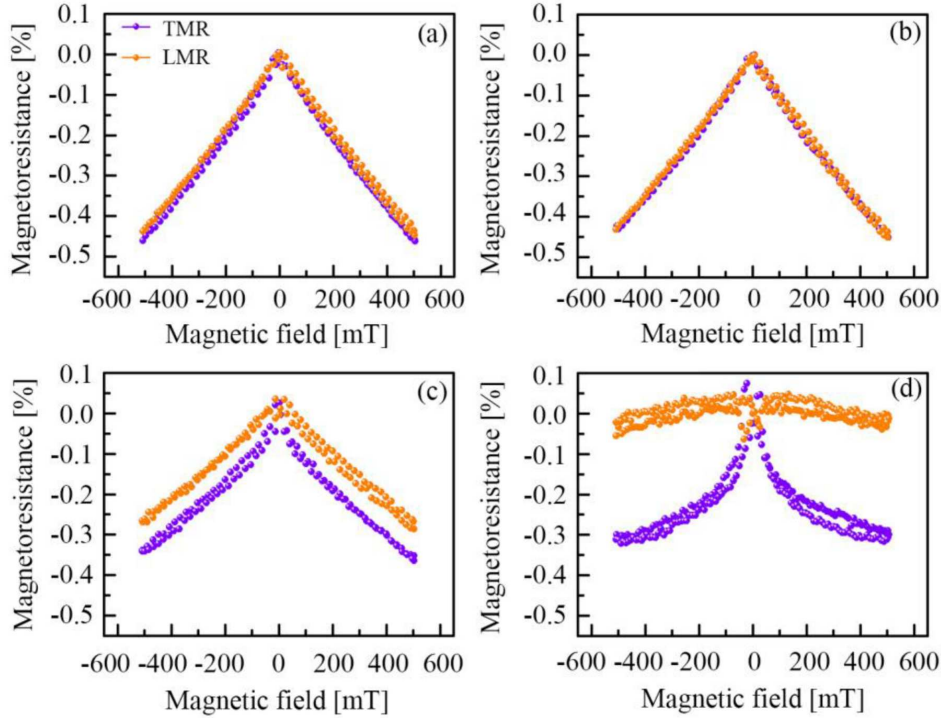


Fig. 5. Field dependences of longitudinal (LMR) and transverse (TMR) magnetoresistance for  $(\text{Ni}_{80}\text{Fe}_{20})_x\text{Au}_{1-x}$  thin films at  $d = 45$  nm and  $c_{\text{Au}} = 30$  at.% annealed to 400 (a), 500 (b), 600 (c), and 700 K (d).

dependences of LMR and TMR of the sample after annealing to various temperatures are presented in Fig. 5. The resulting curves of longitudinal and transverse MR as a function of annealing temperature are shown in Fig. 6. From these curves, it can be found that the growth of magnitude of MR is insignificant upon annealing up to 400 K and 500 K. This behavior can be explained by the following physical viewpoints. According to the TEM investigation, the ferromagnetic grain weakly grows due to the presence of a non-magnetic matrix in their grain boundaries and the low thickness of the samples. As a result, the condition of spin-dependent electron scattering does not change appreciably. Hence, the shape of the  $\text{TMR}(B)$  and  $\text{LMR}(B)$  curves stay unchanged (Fig. 5a and b), and the nature of magnetoresistance remains isotropic. A growth of temperature of annealing to 600 K causes the gradual appearance of anisotropy at the  $\text{MR}(B)$  curves (Fig. 5c). The magnetoresistance anisotropy emergence is caused by the growth and coalescence of ferromagnetic granules. With the increase in annealing temperature up to 700 K, the isotropy at field dependence of magnetoresistance has vanished completely. The anisotropic behavior of magnetoresistance is observed. Upon high-temperature annealing, the number of isolated ferromagnetic granules decreases significantly, giving rise to the reduction of spin-dependent interface scattering. On the other hand, the growth of the size of ferromagnetic clusters increases the possibility of the process

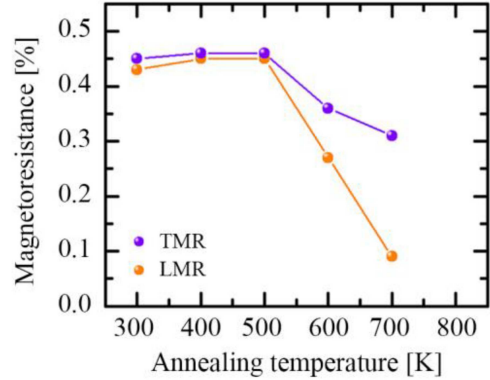


Fig. 6. Magnetoresistance as a function of the annealing temperature for  $(\text{Ni}_{80}\text{Fe}_{20})_x\text{Au}_{1-x}$  thin-film at  $c_{\text{Au}} = 30$  at.% and  $d = 45$  nm.

of electron-phonon scattering. The pass of charge carriers by granules prevents this scattering mechanism. Hence, the probability of spin-dependent electron scattering is reduced.

To obtain more detailed analyses of GMR changes under annealing, we analyzed the changes of resistivity  $\rho$  and  $R_0 - R_{\text{max}}$  with an annealing temperature growth (Fig. 7). We used a value of the resistivity after cooling from a given  $T_{\text{ann}}$  to room temperature as  $\rho$ ;  $R_0$  and  $R_{\text{max}}$  are the resistance in the fields of  $B_0$  and  $B_{\text{max}}$ , respectively. As shown in Fig. 7a, the value of resistivity irreversibly

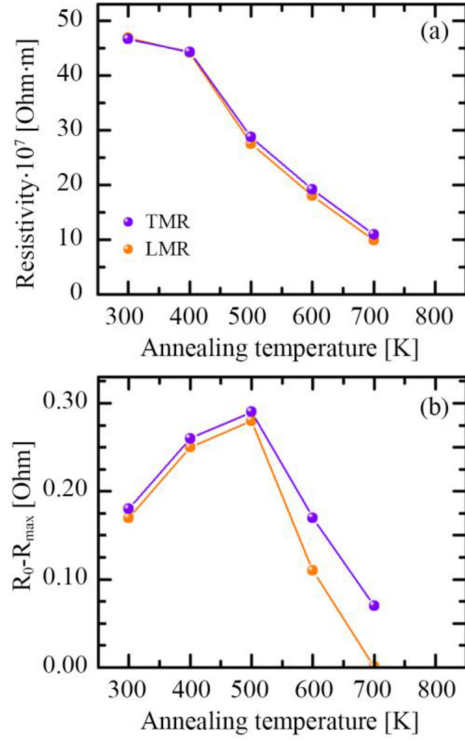


Fig. 7. Resistivity (a) and  $R_0 - R_{max}$  (b) as a function of the annealing temperature for thin-film  $(\text{Ni}_{80}\text{Fe}_{20})_x\text{Au}_{1-x}$  at  $c_{\text{Au}} = 30$  at.% and  $d = 45$  nm.

decreases 4.6 times with the increase in annealing temperature. Such fall is a result of healing defects and the recrystallization process in thin films. Simultaneously, the value of  $R_0 - R_{max}$  first increases 1.6 times and then decreases with  $T_{ann}$ . The rise of  $R_0 - R_{max}$  value within the annealing temperature range 300–500 K can be explained by changing conditions of the spin-dependent electron scattering. The combination of changes in values of  $\rho$  and  $R_0 - R_{max}$  at  $T_{ann} = 300$ –500 K leads to the growth of GMR. The increase in  $T_{ann}$  up to 700 K causes a decrease in resistivity and the value of  $R_0 - R_{max}$ , so the MR ratio goes down. Note that MR ratio has the same changing tendency as  $R_0 - R_{max}$ , indicating that magnetic resistivity  $R_0 - R_{max}$  is directly responsible for the GMR effect.

#### 4. Conclusions

In this article, concentration and annealing affecting the magnetoresistive properties of the nanostructured  $(\text{Ni}_{80}\text{Fe}_{20})_x\text{Au}_{1-x}$  thin film containing from 10 to 60 at.% of Au were investigated. The correlation between crystal structure and magnetoresistive properties of samples with a thickness of 45 nm was studied. Such studies for systems based on  $\text{Ni}_{80}\text{Fe}_{20}$  and Au with a wide range of component concentrations prepared by a co-evaporation method are practically absent in previously reported work.

In diffraction images, for samples as-deposited and annealed at 700 K, there are two fcc lattices, namely, fcc- $\text{Ni}_3\text{Fe}$  and fcc-Au. According to TEM investigations, all samples consist of magnetic granules surrounded by an Au matrix. Peculiarities of the morphology of the samples lead to the isotropic magnetoresistance appearing at  $c_{\text{Au}} = 21$ –46 at.%. The magnitude of the GMR effect reached a maximum at  $c_{\text{Au}} = 30$  at.% and insignificant growth upon annealing up to 400 K and 500 K. The transition to anisotropic magnetoresistance is observed upon annealing to 600 K. The growth of grains during annealing increases the probability of the process of electron-phonon scattering, prevents electron transmission from one ferromagnetic granule to another, and declines the probability of spin-dependent electron scattering.

It is also worth noting that a detailed analysis of the influence of the annealing temperature on the magnitude of the magnetoresistance was carried out for nanostructured  $(\text{Ni}_{80}\text{Fe}_{20})_x\text{Au}_{1-x}$  thin film. For this purpose, the dependences of the value of the specific resistance and the value of  $\Delta R$  on the annealing temperature were obtained. The analysis of these dependences makes it possible to correctly analyze the reasons for the change in the magnitude of the magnetoresistance after annealing.

#### References

- [1] S. Majumdar, R. K. Singha, J. Yoon, M.H. Jung, M. Chakraborty, A.K. Das, S.K. Ray, *Physica B* **404**, 1858 (2009).
- [2] S. Dhara, R. Roy Chowdhury, S. Lahiri, P. Ray, B. Bandyopadhy, *J. Magn. Magn. Mater.* **374**, 647 (2015).
- [3] J. Milano, A.M. Llois, L.B. Steren, *Physica B Cond. Matter.* **354**, 198 (2004).
- [4] S. Arana, N. Arana, F.J. Gracia, E. Castano, *Sens. Actuat. A* **123–124**, 116 (2005).
- [5] Katsuaki Sato, Eiji Saitoh, *Spintronics for Next Generation Innovative Devices*, 2015, p. 255.
- [6] L. Jogschies, D. Klaas, R. Kruppe, J. Rittinger, P. Taptimthong, A. Wienecke, L. Rissing, M.C. Wurz, *Sensors* **15**, 28665 (2015).
- [7] Changzheng Wang, Zhenghong Guo, Yonghua Rong, T.Y. Hsu (Xu Zuyao), *J. Magn. Magn. Mater.* **277**, 273 (2004).
- [8] M. Tamisari, F. Spizzo, M. Sacerdoti, G. Battaglin, F. Ronconi, *J. Nanopart. Res.* **13**, 5203 (2011).
- [9] J.M. Soares, J.H. de Araújo, F.A.O. Cabral, F.L.A. Machado, T. Dumelow, M.M. Xavier Jr., J.M. Sasaki, *J. Non-Cryst. Solids* **354**, 4883 (2008).

- [10] N.M. Sugihiro, W.S. Torres, W.C. Nunes, E.B. Saitovitch, M.R. Mc Cartney, D.J. Smith, A.M.L.M. Costa, I.G. Solórzano, *Mater. Chem. Phys.* **266**, 124517 (2021).
- [11] I.O. Shpetnyi, K.V. Tyschenko, V.Ya. Pak, B.V. Duzhyi, Yu.O. Shkurdoda, I.Yu. Protsenko, *J. Nano- Electron. Phys.* **13**, 01020 (2021).
- [12] I.M. Pazukha, O.V. Pylypenko, L.V. Odnodvoretz, *Mater. Res. Express* **5**, 106409 (2018).
- [13] I.O. Shpetnyi, S.I. Vorobiov, D.M. Kondrakhova, M.S. Shevchenko, L.V. Duplik, L.V. Panina, V.I. Grebinaha, Yu.I. Gorobets, L. Satrapinsky, T. Lucinski, *Vacuum* **176**, 109329 (2020).
- [14] D. Samal, D. Venkateswarlu, P.S. Anil Kumar, *Solid State Commun.* **150**, 576 (2010).
- [15] L.V. Odnodvoretz, I.Yu. Protsenko, Yu.M. Shabelnyk, M.O. Shumakova, O.P. Tkach, *J. Nano- Electron. Phys.* **8**, 03034 (2016).
- [16] S. Bogatyrenko, A. Kryshchal, A. Minenkov, A. Kruk, *Scr. Mater.* **170**, 57 (2019).
- [17] Jorge A. Muñoz, Brent Fultz, *AIP Conf. Proc.* **1671**, 020001 (2015).
- [18] O.V. Pylypenko, I.M. Pazukha, A.S. Ovrytskyi, L.V. Odnodvoretz, *J. Nano- Electron. Phys.* **8**, 03022 (2016).
- [19] Changzheng Wang, Xiaoguang Xiao, Haiquan Hu, Yonghua Rong, T.Y. Hsu, *Physica B* **392**, 72 (2007).
- [20] E. Rozenberg, A.I. Shames, G. Gorodetsky, J. Pelleg, I. Felner, *J. Magn. Magn. Mater.* **203**, 102 (1999).
- [21] A.N. Pohorilyi, A.F. Kravets, E.V. Shypil', D.Y. Pod'yalovsky, A.Ya. Vovk, Chang Sik Kim, M.V. Prudnikova, H.R. Khan, *Thin Solid Films* **423**, 218 (2003).
- [22] B. Dieny, S.R. Teixeira, B. Rodmacq, C. Cowache, S. Auffret, O. Redonand, J. Pierre, *J. Magn. Magn. Mater.* **130**, 197 (1994).